EXHIBIT T

Loss of stability by migration and chemical reaction of Santonox (R) R in branched polyethylene under anaerobic and aerobic conditions

Article *in* Polymer Degradation and Stability · May 2006

DOI: 10.1016/j.polymdegradstab.2005.07.010

Available online at www.sciencedirect.com
SCIENCE DIRECT
Polymer Degradation and Stability 91 (2006) 1071–1078
Polymer Degradation and Stability
www.elsevier.com/locate/polydegstab

Loss of stability by migration and chemical reaction of Santonox® R in branched polyethylene under anaerobic and aerobic conditions

M. Lundbäck, C. Strandberg, A.-C. Albertsson, M.S. Hedenqvist, U.W. Gedde*

School of Chemical Science and Engineering, Fibre and Polymer Technology, Royal Institute of Technology, SE-100 44 Stockholm, Sweden

Received 30 May 2005; received in revised form 7 July 2005; accepted 25 July 2005
Available online 15 September 2005

Abstract

Plaques of branched polyethylene stabilized with 0.1 wt.% 4,4′-thiobis(6-*tert*-butyl-3-methylphenol) [Santonox® R] were aged at different temperatures between 75 and 95 °C in anaerobic (nitrogen or water) and aerobic (air or water saturated with air) media. Antioxidant concentration profiles were obtained by oxidation induction time (OIT) measurements using differential scanning calorimetry. Results obtained by high performance liquid chromatography of extracts confirmed that the gradual decrease in OIT with increasing ageing time was due to migration of antioxidant to the surrounding medium. The antioxidant concentration profiles along the plaque thickness direction were flat in the plaques aged in the non-aqueous media indicating that the migration of antioxidant to the surrounding medium was controlled by the low evaporation rate at the material boundary. Crystals of antioxidant were detected by optical microscopy on the samples exposed to nitrogen. The similarity of the antioxidant concentration profiles obtained after ageing in nitrogen and in air suggested that the fraction of the antioxidant oxidized is negligible in comparison with the loss of antioxidant by migration to the surrounding media. The antioxidant concentration profiles along the plaque thickness direction obtained after ageing in water were less flat, suggesting faster dissolution in the water phase than evaporation in the case of non-aqueous ageing. The antioxidant diffusivity could be determined from the aqueous experiments and was in reasonable agreement with data reported by Moisan. For the samples exposed to water, the loss of antioxidant was faster from the samples exposed to water saturated with air. This difference is attributed to a faster degradation of the antioxidant in the oxygen-containing water phase increasing the mass transport from the polymer phase boundary to the water phase.

Keywords: Branched polyethylene; Chemical consumption; Migration; Santonox R

1. Introduction

The loss of antioxidant protection of polymers is an important topic addressed in a large number of scientific and technical reports. The migration of antioxidant to the surrounding media ('physical loss') and the oxidation of the antioxidant ('chemical consumption') are two important mechanisms for the loss of stability [1–3]. The physical loss of antioxidant is controlled either by the rate of diffusion of the antioxidant in the polymer or by its escape rate at the material boundary. The latter can be due to either evaporation in a gas phase medium or dissolution in a liquid phase like water. Gedde et al. [4,5] reported data for polyolefin hot-water pipes suggesting that the chemical consumption of phenolic antioxidants was negligible compared to the physical loss of antioxidant at temperatures between 70 and 110 °C. Billingham [1] has also shown the significance of physical loss for the loss in stability of polyolefins.

* Corresponding author. Tel.: +46 8 7907640; fax: +46 8 208856.
E-mail address: gedde@polymer.kth.se (U.W. Gedde).

0141-3910/$ - see front matter © 2005 Elsevier Ltd. All rights reserved.
doi:10.1016/j.polymdegradstab.2005.07.010

This paper is a follow-up of earlier papers by Gedde et al. [4–10]. The material studied and the ageing conditions are simplified in comparison with the previous studies: (i) the polymer contained only a single antioxidant (Santonox R) of known initial concentration, (ii) well-defined ageing conditions were used – oxygen-free nitrogen or oxygen-free water (anaerobic conditions); air or water saturated with air (aerobic conditions). These more precisely controlled experiments enabled different loss mechanisms to be assessed. The antioxidant concentration profiles were obtained by measurement of the oxidation induction time (OIT) by differential scanning calorimetry. Extracts were analyzed by high performance liquid chromatography to confirm that the decrease in OIT was due to migration of antioxidant to the surrounding medium rather than to internal precipitation of the antioxidant [10].

A model based on Fick's second law with a one-parameter description of the outer boundary conditions was used to fit the experimental antioxidant concentration profiles. The escape rate at the outer boundaries was in some cases significantly lower than the diffusion rate, and this resulted in very 'flat' antioxidant concentration profiles. The assessment of the diffusivity in these cases was impossible. The antioxidant diffusivities obtained from the 'good' cases have been compared with data reported earlier by Moisan [11] using a different method for the assessment of antioxidant diffusivity.

A comparison of the loss of antioxidant protection under anaerobic and aerobic conditions confirmed that the proportion of antioxidant lost by chemical consumption in the polymer phase was negligible in comparison with the loss by migration to water. Interestingly, the physical loss to water was faster under aerobic than under anaerobic conditions.

2. Experimental

2.1. Materials

The antioxidant, Santonox R [4,4′-thiobis(6-*tert*-butyl-3-methylphenol)], was kindly supplied by Monsanto Inc., USA and the branched polyethylene (grade code BCM 1912) without stabilizer was obtained from Borealis AB, Sweden. Characteristics of this polyethylene: density = 919 kg m^{-3} (mass crystallinity = 48%; obtained by using the specific volume data for crystalline and amorphous polyethylene according to Wunderlich [12]); $\bar{M}_n = 29.3$ kg mol^{-1}; $\bar{M}_w = 104$ kg mol^{-1}; the branches were exclusively ethyl branches. The molar mass data were obtained by size exclusion chromatography (Polymer Laboratories GPC 220 equipped with a refractive index detector using 1,2,4-trichlorobenzene as solvent and the universal calibration procedure).

2.2. Sample preparation

The antioxidant was dissolved in dichloromethane at room temperature and added to the polyethylene powder. The mixture of solvent, antioxidant, and PE powder was stirred continuously until the solvent had evaporated. The concentration of antioxidant in the dry powder blend was 0.1 wt.%. Plaques (100 × 100 × 2.7 mm) were obtained by compression moulding using a Swabenthan Polystat 300 S compression-moulding machine at 140 °C for 11 min holding the pressure at 70 Pa followed by a 10 °C min^{-1} cooling to room temperature while maintaining the pressure. Differential scanning calorimetry (Mettler Toledo 820, sample mass: 6.5 ± 0.3 mg) showed that the moulded plaque samples had a melting point of 124 °C and a mass crystallinity of 50%.

2.3. Ageing

The moulded plaques were cut into samples of 3 × 9 cm^2 (edges were removed from the moulded plaque) and kept in glass containers in a temperature-calibrated Memmert ULE600 oven equipped with a fan. The temperature at all specimen positions was within 0.5 °C of the target temperature. The specimens were aged at 75, 90 and 95 °C.

Anaerobic ageing was performed using two conditions: nitrogen gas or water with a constant flow of nitrogen gas (45 ± 5 ml min^{-1}) in the glass containers. The oxygen content of the flushing nitrogen gas was measured with a PBI-Dansensor to be less than 0.065 vol.%. The gas coming from gas tubes outside the oven was led through metal pipes in spirals inside the oven to achieve temperature control of the gas.

Aerobic ageing was performed using two conditions: exposure to air or to water saturated with air by a constant flow of air (45 ± 5 ml min^{-1}) from the bottom of the glass containers.

Aqueous ageing was performed with six samples (each sample weighing approximately 8 g) stored in 3 l of distilled water. The water was replaced thrice – after one, two and three weeks of exposure. The maximum concentration of Santonox R in the water phase was typically 5 ppm.

2.4. Oxidation induction time (OIT) measurements

Cylindrical samples with a diameter of 5 mm were punched from the plaques. Thin sections (0.1–0.15 mm thick) were obtained using a Leica Jung Autocut 2055 from the cylindrical punched samples. The thermal analyses were performed in a Mettler Toledo DSC820 analyzing three sections, 0.1–0.15 mm thick and 5 mm in diameter with a total mass of 5 ± 1 mg. The sections were enclosed in an aluminium pan (40 μl) encapsulated

with a lid with three holes (each hole was 1 mm in diameter) to allow transport of oxygen to the sample. The oxidation induction time (OIT) measurements were performed by heating the samples to 200 °C at a rate of 100 °C min^{-1} and then maintaining the sample at 200 °C. The purge gas was oxygen at a flow rate of 80 ml min^{-1} throughout the experiment. The consumption of antioxidant during the non-isothermal period was negligible. The oxidation induction time was obtained as the intersection between the isothermal base line and the tangent to the curve at the point which deviated exothermally by 1 mW from the isothermal base line.

2.5. Extraction

Samples based on a number of 0.1–0.15 mm thick slices weighing a total of 1.5 g were Soxhlet extracted for 5 h in 100 ml chloroform. The extraction solutions were filtered through 0.45 μm PTFE filters before further analysis.

Microwave-assisted extractions were performed in standard vessels with an inner diameter of 30 mm using a Microwave Extraction System, model MES-1000 from CEM Corporation, with a nominal power of 1 kW. The sample, which consisted of 0.1–0.15 mm thick slices weighing a total of 100–130 mg, was mixed with 10 ml of acetonitrile and a small amount of Irganox 1010, 0.01 mg (ml)$^{-1}$ in the final solution as internal standard. The extractions were carried out by heating from 25 to 80 °C during 6 min at 0.75 kW power, followed by further heating to 100 °C during 4 min at 1 kW and finally maintaining at this temperature for 30 min at 0.9 kW.

2.6. High performance liquid chromatography

Samples were analyzed with a Hewlett Packard series 1100 HPLC with a deuterium UV-detector and a Shimadzu pump LC-10AD. The antioxidant concentration was determined by reversed-phase HPLC, with acetonitrile–water (95/5) as the mobile phase and a Waters Symmetry C18 column (50 × 390 mm, 5 μm). The concentration of antioxidant was determined from the absorption at 220 nm. An injection volume of 10 μl and a flow rate of 0.5 ml min^{-1} were used. The extraction solutions were filtered through 0.45 μm PTFE filters before the analysis. Duplicate measurements were made for each sample.

The solutions obtained by Soxhlet extraction were analyzed with normal-phase HPLC on a Hewlett Packard Chromatograph, HPLC 1090, equipped with a binary pump system, an M490 variable wavelength UV detector, a Waters model 990 diode array detector and a WISP autosampler. The antioxidant concentration was determined on a Supelcosil column (4.5 × 150 mm, 5 μm) with chloroform at 0.5 ml/min as the mobile phase at a wavelength of 280 nm.

2.7. Optical microscopy

Samples exposed to nitrogen at elevated temperatures were examined in a Nikon 50 W AD optical microscope.

3. Results and discussion

3.1. Antioxidant loss

The OIT profiles displayed in Figs. 1–3 represent only half the pipe wall, 1.4 mm out of the total 2.8 mm. The same external medium was present on both sides of the plaque specimens and the antioxidant profiles were symmetrical about the centre of the pipe wall. The OIT profile of the unexposed plaque showed a ~30% lower value at the outer boundaries with respect to the centre value (Figs. 1–3). This suggests that part of the antioxidant was lost by evaporation during the moulding of the plaques. The dispersion of the antioxidant seems good in view of the low scatter of the OIT data at different depths in the unexposed plaque.

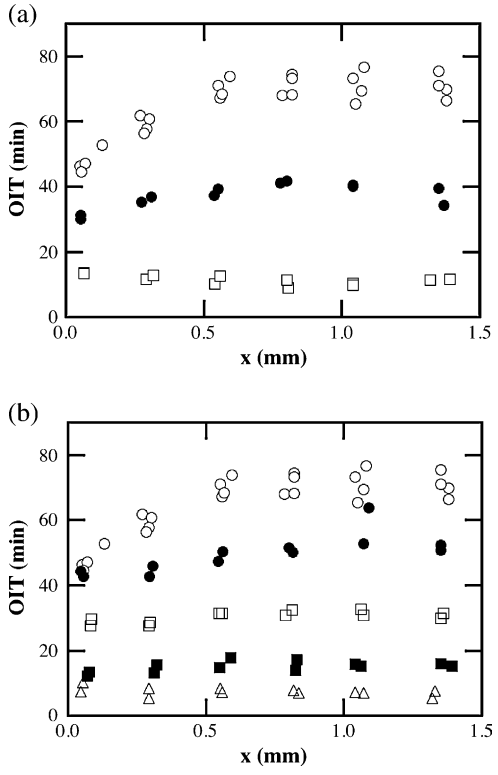

Fig. 1. Oxidation induction time (OIT) profiles in plaques exposed to oxygen-free water at different temperatures: (a) 75 °C: ○ unexposed, ● 408 h, □ 1008 h. (b) 90 °C: ○ unexposed, ● 240 h, □ 624 h, ■ 984 h, △ 1320 h.

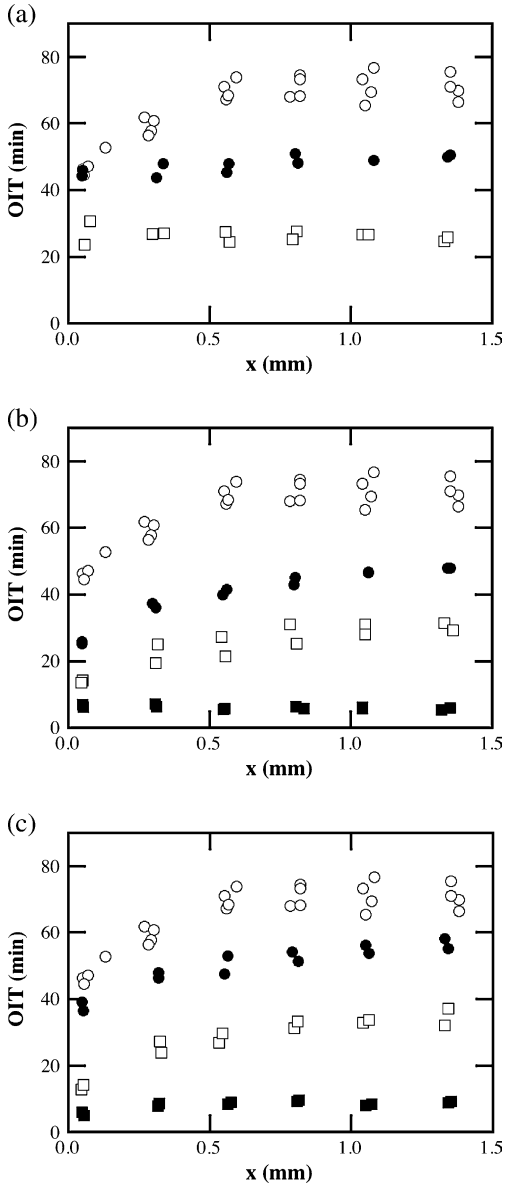

Fig. 2. Oxidation induction time (OIT) profiles in plaques exposed to water saturated with air at different temperatures: (a) 75 °C: ○ unexposed, ● 456 h, □ 1104 h. (b) 90 °C: ○ unexposed, ● 48 h, □ 120 h, ■ 456 h. (c) 95 °C: ○ unexposed, ● 24 h, □ 72 h, ■ 240 h.

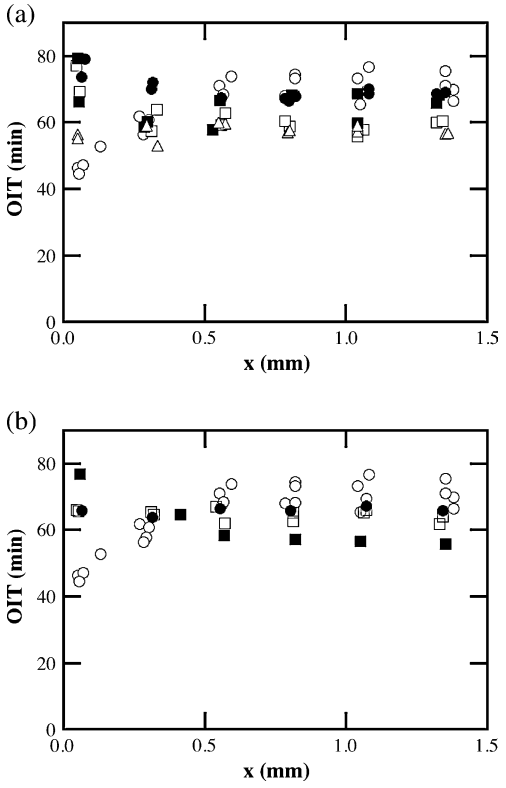

Fig. 3. (a) Oxidation induction time (OIT) profiles in plaques exposed to nitrogen at different temperatures for different periods of time: ○ unexposed, ● 10 848 h at 75 °C, □ 16 728 h at 75 °C, ■ 7728 h at 90 °C, △ 7728 h at 95 °C. (b) Oxidation induction time (OIT) profiles from plaques exposed to air at different temperatures for different periods of time: ○ unexposed, ● 2304 h at 75 °C, □ 6984 h at 90 °C, ■ 2304 h at 95 °C.

The OIT data remained within a 10% band about the mean value.

Fig. 1 presents OIT profiles from the plaques aged in oxygen-free water. The initial curved OIT profile became more flat on ageing and the concentration at the boundary was only 5–15% lower than that in the centre of the plaque wall. The curve shape suggests that the migration of antioxidant to the surrounding water was limited by the slow dissolution of the antioxidant in water. The OIT profiles of the plaques exposed to water saturated with air showed a greater curvature even after extended ageing (Fig. 2). The OIT value at the boundary of these samples was significantly lower than that in the centre, indicating that the dissolution of antioxidant was facilitated by the presence of oxygen in the water phase. Ageing in non-aqueous media (nitrogen or air) led to practically no reduction in OIT (Fig. 3). The initially curved OIT profile became completely flat on ageing in both media and the presence of oxygen in air has no measurable impact on the OIT profiles (Fig. 3).

The surfaces of the specimens aged in nitrogen for long periods of time were examined in the optical microscope, and it was found that the outer surface was covered with blooming antioxidant crystals (Fig. 4). The migration of low molar mass species to the surface was also evident for these samples in the waxy character of the surface. The surface became waxy after exposure due to migration from the bulk of low molar mass species.

Fig. 5 presents the average OIT (averaging through the plaque wall) as a function of the square root of the exposure time after ageing in the different media. Ageing in the non-aqueous media led to practically no decrease in OIT, and the difference in OIT between anaerobic and aerobic non-aqueous ageing was insignificant. Aqueous ageing, on the other hand, resulted in

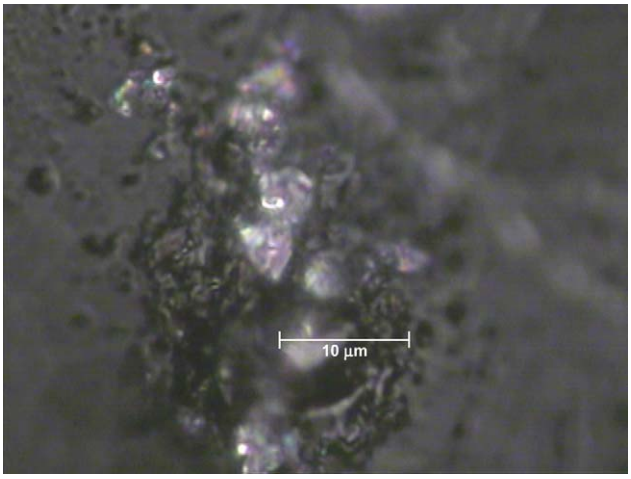

Fig. 4. Photomicrograph of the waxy surface on the plaque exposed to nitrogen at 90 °C for 7728 h. The blooming antioxidant crystals reflect the light.

a significantly more rapid decrease in OIT. The fastest decrease in OIT was obtained for the samples aged in oxygen-containing water.

3.2. High performance liquid chromatography (HPLC) on extracts

The antioxidant in unaged, stabilized polymer with 0.1 wt.% antioxidant was isolated from the polymer using either microwave-assisted extraction (MAE) or Soxhlet extraction. The residual antioxidant concentration was determined by HPLC and the Soxhlet extraction recovered more antioxidant (0.092 wt.%) than MAE (0.076 wt.%). The small difference between the nominal antioxidant concentration (0.1 wt.%) and the antioxidant concentration obtained by HPLC on the Soxhlet extract suggests that a small part of the antioxidant was lost during sample preparation (mixing and moulding). HPLC on solutions obtained by MAE was used to study the loss of antioxidant from the polymer during ageing, despite the fact that the extraction method recovered less antioxidant from the polymer than Soxhlet extraction.

Chromatograms of the extraction solutions obtained by MAE of samples from plaques aged in oxygen-free water at 90 °C are displayed in Fig. 6. The peak associated with Santonox R decreased gradually with increasing ageing time. There was no trace of antioxidant in the sample aged for 5856 h and, most important, the OIT result for the similar sample was 0 min. These data prove that the antioxidant migrated to the surrounding medium during this ageing time and that no internal phase separation of the antioxidant occurred in the polymer phase according to the Regime A mechanism [10].

Fig. 7 shows that the antioxidant concentration increased with increasing OIT. The data showed a positive curvature, which is unexpected based on earlier experience of similar antioxidants [13]. The deviation of the single data points from a straight line is relatively small and it is suggested that the curvature may be due to the uncertainty caused by the inefficiency of the MAE method used. The OIT data reported in this paper are assumed to be proportional to the antioxidant concentration in the polymer.

3.3. Analysis of antioxidant concentration profiles

The diffusivity and the boundary loss kinetics of the antioxidant were estimated by fitting the profiles of the antioxidant concentration within the plaques. The fitting

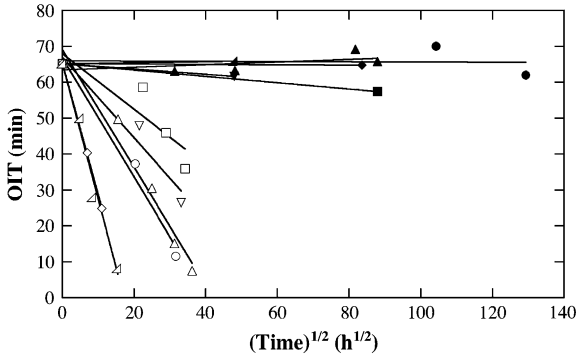

Fig. 5. The average OIT values of the antioxidant profiles at different exposure times for samples exposed to different media at different temperatures versus the square root of time in hours: ● N_2 75 °C; ▲ N_2 90 °C, ■ N_2 95 °C; ▼ air 75 °C, ◆air 90 °C, ◢ air 95 °C; ○ $H_2O(N_2)$ 75 °C; △ $H_2O(N_2)$ 90 °C; □ $H_2O(N_2)$ 95 °C; ▽ H_2O(air) 75 °C; ◇ H_2O(air) 90 °C; ◿ H_2O(air) 90 °C.

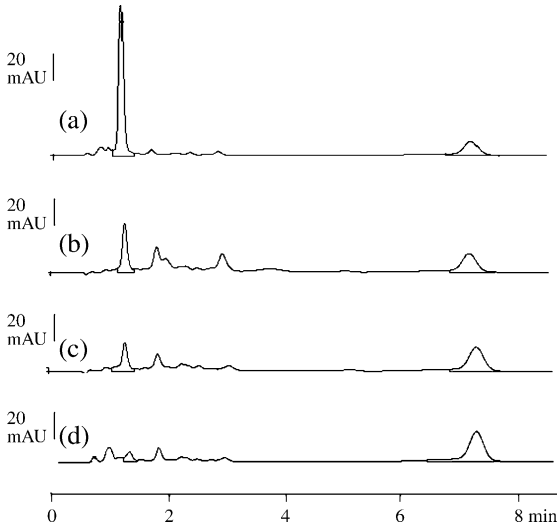

Fig. 6. HPLC chromatograms of extracted solutions from plaques exposed to oxygen-free water at 90 °C for different periods of time: (a) unexposed; (b) exposed 240 h; (c) 624 h; (d) 5856 h. The peak appearing at 1.3 min is from Santonox R and the peak at 7.3 min is from the internal standard (Irganox 1010).

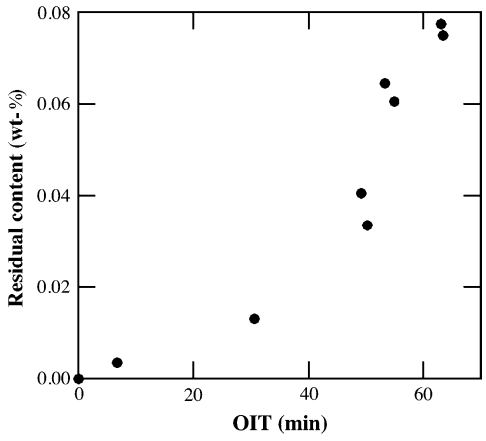

Fig. 7. Antioxidant concentration in wt.% obtained by HPLC as a function of the oxidation induction time (OIT) of samples exposed to oxygen-free water at 90 °C.

was achieved using the successive over-relaxation method (SOR). SOR was chosen because it is more efficient than the Crank–Nicholson method [14]. The antioxidant diffusivity (D) was assumed to be independent of the antioxidant concentration, and the boundary loss rate (F_0) was obtained by fitting the system of equations to the experimental data using a simplex-search algorithm.

The mass transfer of antioxidant is expressed as [15]:

$$\frac{\partial C}{\partial t}=\frac{\partial}{\partial x}\left(D\frac{\partial C}{\partial x}\right) \tag{1}$$

where C is the antioxidant concentration and x is the distance from the outer wall. Eq. (1) is discretized throughout the thickness according to:

$$\frac{\partial C}{\partial t}=\frac{D}{\Delta x_i^2}[(C_{i+1}-2C_i+C_{i-1})] \tag{2}$$

The loss of antioxidant at the plaque surface is described by:

$$D\left[\frac{\partial C}{\partial x}\right]_{x=0}=F_0C \tag{3}$$

which may be written explicitly as ($i=0$ at the surface):

$$C_0=\frac{C_1}{1+\frac{\Delta x_i F_0}{D}} \tag{4}$$

The generalized iterative scheme for solving $\bar{C}$, the concentration vector, at each time step is $\bar{A}\bar{C}_{j+1}=\bar{b}$. In this equation, $\bar{A}$ is the three-diagonal Jacobian matrix which, in the case of the Crank–Nicholson scheme, is given by:

$$\bar{A}=\begin{pmatrix} 2(1+r) & -r & & & \\ -r & 2(1+r) & -r & & \\ & & \dots & & \\ & & -r & 2(1+r) & -r \\ & & & -r & 2(1+r) \end{pmatrix} \tag{5}$$

The elements not displayed in the matrix in Eq. (5) are zero and $r=(\Delta t/\Delta x^2)D$; $\bar{b}$ is the vector with the known solution in the previous time step j: $\bar{b}=r\bar{C}_{i-1,j}+2(1-r)\bar{C}_{i,j}+r\bar{C}_{i+1,j}$. The iterative scheme of the successive over-relaxation method is

$$\bar{C}_{j+1}^{(n+1)}=\bar{C}_{j+1}^{(n)}+\omega\Delta\bar{C}_{j+1}^{(n)} \tag{6}$$

where

$$\Delta\bar{C}_{j+1}^{(n)}=\frac{1}{2(1+r)}\left\{\bar{b}-\bar{L}\bar{C}_{j+1}^{(n+1)}-[\bar{M}+2(1+r)\bar{I}]\bar{C}_{j+1}^{(n)}\right\} \tag{7}$$

$\bar{A}$ is the Jacobian matrix in Eq. (5) with the components in the central diagonal equal to zero and $\bar{L}$ and $\bar{M}$ are, respectively, the lower and upper parts of $\bar{A}$, i.e. $\bar{A}=\bar{L}+\bar{M}$. The convergence of SOR is highly dependent on the value of ω, which should be between 1 and 2. Its value (ω_{opt}) for the optimum speed of convergence is given by:

$$\omega_{opt}=\frac{2}{1+\left(1-\left[\frac{r}{1+r}\cos\left(\frac{\pi}{N}\right)\right]^2\right)^{0.5}} \tag{8}$$

The program, which searches for the optimum parameter values describing loss rate at the polymer boundary (F_0) and the antioxidant diffusion (D) by fitting the above equations to the antioxidant concentration profiles, was only successful in the case of aqueous ageing. The antioxidant concentration profiles of the plaques aged under water-free conditions were flat as illustrated by Fig. 3, showing that the migration of antioxidant was controlled by the slow evaporation. The loss of antioxidant was the same in air as in nitrogen, which indicated that the oxidative consumption of antioxidant in the polymer phase was negligible.

Fig. 8 shows two experimental OIT profiles together with an adequate fitting of Eqs. (1) and (3) to the experimental data. Some of the OIT profiles were relatively flat, in particular those obtained after ageing in anaerobic water. The fittings of the diffusion and the boundary loss equations were associated with considerable uncertainty in these cases. Ageing in aerobic water yielded antioxidant concentration profiles with more curvature (Figs. 1 and 2), more suited for modelling and more

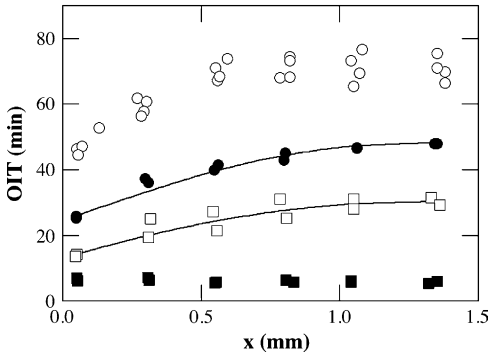

Fig. 8. Oxidation induction time (OIT) profiles from plaques exposed to water saturated with air at 90 °C. The experimental results are presented as: ○ unexposed, ● 48 h, □ 120 h. The continuous lines are best fits of Eqs. (1) and (3) to the experimental data.

precise determination of the antioxidant diffusivity and the boundary loss rate.

The results of the fittings are presented in Table 1. The antioxidant diffusivity showed essentially the same dependence on temperature in both anaerobic and aerobic water. The boundary loss rate, however, was different, depending on the surrounding medium. The boundary loss rate increased only moderately with increasing temperature for ageing in anaerobic water, whereas it increased markedly with increasing temperature in aerobic water. This is consistent with the difference in the OIT profiles presented in Figs. 1 and 2. The ratio between the boundary loss rate and the diffusivity remained essentially constant (50 ± 4) for ageing in anaerobic water. In the case of ageing in aerobic water, it increased from 48 ± 1 at 75 °C to 80 ± 5 at 95 °C. The consumption of antioxidant by oxidation was insignificant, according to the data obtained from ageing in the different non-aqueous media. The relatively rapid loss of stability in aerobic water is attributed to a high boundary loss rate, which can be tentatively explained by oxidation of the antioxidant in the water phase. Mikami et al. [16] presented evidence for free-radical oxidation of BHT in water saturated with air.

Table 1
Parameters obtained by fitting Eqs. (1) and (3) to the experimental antioxidant concentration profiles

Medium, T (°C)	Exposure time (h)	$F_0 \times 10^7$ (cm s^{-1})	$D \times 10^8$ (cm^2 s^{-1})	F_0/D (cm^{-1})
H_2O(air), 75	456	9	1.9	48
H_2O(air), 75	1104	9	1.8	49
H_2O(air), 90	48	33	4.7	71
H_2O(air), 90	120	25	3.1	80
H_2O(air), 95	72	36	4.1	87
H_2O(air), 95	240	31	4.3	73
$H_2O(N_2)$, 75	408	10	1.9	52
$H_2O(N_2)$, 75	1008	12	2.1	56
$H_2O(N_2)$, 90	240	12	2.5	49
$H_2O(N_2)$, 90	624	19	4.0	48
$H_2O(N_2)$, 90	984	9.5	1.7	55
$H_2O(N_2)$, 95	840	15	3.3	46
$H_2O(N_2)$, 95	1176	17	3.7	47

Fig. 9 shows the diffusivity as a function of inverse temperature (Arrhenius diagram) including data from both anaerobic and aerobic water ageing. The large scatter in the data makes an accurate assessment of the activation energy impossible: 40 ± 30 kJ mol^{-1} (including all data); 50 ± 30 kJ mol^{-1} (including only data from samples aged in water saturated with air). The higher boundary loss rate in oxygen-containing water made the assessments of the diffusivities more accurate in these cases. Moisan [11] reported an activation energy of 88 kJ mol^{-1} for the diffusion of Santonox R in branched polyethylene. The absolute values of the diffusivities are in reasonably good agreement with data reported by Moisan [11]. At 95 °C: $D \approx 2 \times 10^{-7}$ cm^2 s^{-1} (Moisan) and $0.3–0.4 \times 10^{-7}$ cm^2 s^{-1} (this paper). The antioxidant diffusivity values at 75 °C were even closer: $D \approx 4 \times 10^{-8}$ cm^2 s^{-1} (Moisan) and 2×10^{-8} cm^2 s^{-1} (this paper). It may be concluded that the low boundary loss rate makes the assessment of the antioxidant diffusivity less precise. A relatively small scatter in single OIT data points has a significant effect on the fitted diffusivity.

Fig. 10 shows the boundary loss rate as a function of temperature. The boundary loss rate increased only moderately with increasing temperature in anaerobic water, whereas the boundary loss rate in aerobic water showed a pronounced increase with increasing temperature. In the latter case it obeyed the Arrhenius law with an activation energy of 73 kJ mol^{-1}.

4. Conclusions

Plaques of branched polyethylene stabilized with 0.1 wt.% Santonox R were aged at elevated temperatures

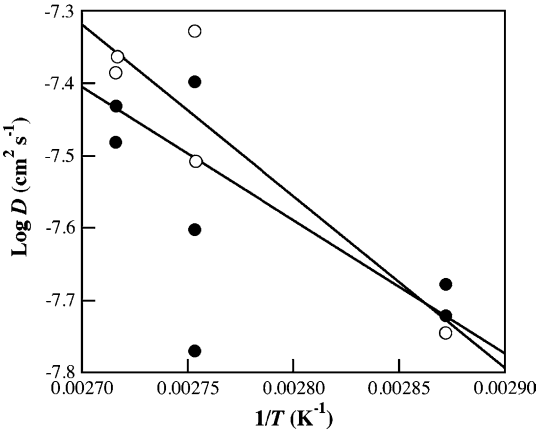

Fig. 9. Antioxidant diffusivity as a function of inverse temperature (Arrhenius diagram). Data are from fitting of Eqs. (1) and (3) to the experimental antioxidant profiles obtained after ageing in aqueous media: ● oxygen-free water; ○ water saturated with air. The lines were obtained by fitting the Arrhenius equation to the experimental data.

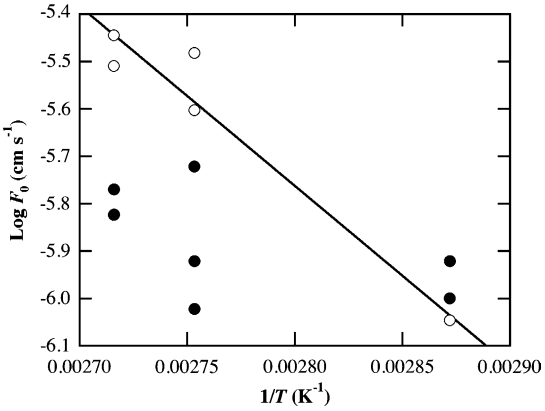

Fig. 10. Boundary loss rate (F_0) as a function of temperature (Arrhenius diagram). Data are from fitting of Eqs. (1) and (3) to the experimental antioxidant profiles obtained after ageing in aqueous media: ● oxygen-free water; ○ water saturated with air. The line was obtained by fitting the Arrhenius equation to the experimental data obtained on samples aged in water saturated with air. The activation energy obtained was 73 kJ mol^{-1}.

(75–95 °C) in anaerobic and aerobic media. The change in antioxidant concentration with time was studied by measurement of the oxidation induction time (OIT). High performance liquid chromatography confirmed that the gradual decrease in OIT with increasing ageing time was due to migration of antioxidant to the surrounding medium. The antioxidant concentration profiles along the plaque thickness direction after non-aqueous ageing were flat, which indicated that evaporation loss determined the migration of antioxidant to the surrounding medium. The presence of oxygen in the non-aqueous medium had no measurable effect on the antioxidant consumption. The antioxidant concentration profiles along the plaque thickness direction were less flat after ageing in aqueous media suggesting that the antioxidant diffusion also affected the migration rate. The rate of dissolution of antioxidant at the plaque boundary was higher, particularly at 90 and 95 °C, in water saturated with air than in oxygen-free water. This difference is attributed to faster degradation of the antioxidant in the oxygen-containing water phase. The low boundary loss rate makes the assessment of the antioxidant diffusivity far from ideal and it is associated with a sizeable uncertainty. However, the antioxidant diffusivities obtained were in fair agreement with data reported by Moisan [11].

Acknowledgements

This work has been sponsored by the Swedish Research Council (grant 621-2001-2321).

References

[1] Billingham NC. In: Scott G, editor. Atmospheric oxidation and antioxidants, vol. 2. Amsterdam: Elsevier; 1993.
[2] Billingham NC, Garcia-Trabajo P. Polym Degrad Stab 1995;48:419.
[3] Pospíšil J, Nešpůrek S. Handbook of polymer degradation. New York: Marcel Dekker; 2000. p. 191.
[4] Viebke J, Gedde UW. Polym Eng Sci 1997;37:896.
[5] Smith GD, Karlsson K, Gedde UW. Polym Eng Sci 1992;32:658.
[6] Gedde UW, Ifwarson M. Polym Eng Sci 1990;30:202.
[7] Viebke J, Elble E, Ifwarson M, Gedde UW. Polym Eng Sci 1994;34:1354.
[8] Viebke J, Elble E, Gedde UW. Polym Eng Sci 1994;36:458.
[9] Gedde UW, Viebke J, Leijström H, Ifwarson M. Polym Eng Sci 1994;34:1773.
[10] Viebke J, Hedenqvist M, Gedde UW. Polym Eng Sci 1996;36:2896.
[11] Moisan JY. Eur Polym J 1980;16:979.
[12] Wunderlich B. Crystal structure, morphology, defects. In: Macromolecular physics, vol. 1. New York: Academic Press; 1974.
[13] Fateh-Alavi K, Karlsson S, Gedde UW. J Appl Polym Sci 2004;93:2185.
[14] Greenberg MD. Advanced engineering mathematics. New Jersey: Prentice-Hall; 1988.
[15] Crank J. The mathematics of diffusion. 2nd ed. Oxford: Oxford University Press; 1975.
[16] Mikami N, Gomi H, Myamoto J. Chemosphere 1979;5:311.